Research Article

Contradictory Effects of Chemical Filters in UV/ROS-Stressed Human Keratinocyte and Fibroblast Cells

Stefanie Hofer [1,2], Marlies Stonig [1], Verena Wally [3], Anja Hartmann [2], Dietmar Fuchs [4], Martin Hermann [5], Martin Paparella [1], Markus Ganzera [2] and Johanna M. Gostner [1]

[1]Division of Medical Biochemistry, Biocenter, Medical University of Innsbruck, Innsbruck, Austria; [2]Institute of Pharmacy/Pharmacognosy, University of Innsbruck, Innsbruck, Austria; [3]EB House Austria, Research Program for Molecular Therapy of Genodermatoses, Department of Dermatology, University Hospital of the Paracelsus Medical University Salzburg, Salzburg, Austria; [4]Division of Biological Chemistry, Biocenter, Medical University of Innsbruck, Innsbruck, Austria; [5]Department of Anaesthesiology and Critical Care Medicine, Medical University of Innsbruck, Innsbruck, Austria

Abstract

Chemical UV filters are frequently applied as active ingredients in sunscreens to protect from detrimental effects of UV radiation. Regardless, many of these compounds are not well characterized concerning their capacity to counteract UV induced reactive oxygen species (ROS). Intracellular ROS release is an early event upon UV exposure and a crucial trigger of reaction cascades that may provoke adverse effects both in the short- and long-term. We report a strategy to assess the capacity of UV filters (ecamsule, oxybenzone, and menthyl anthranilate) to counteract UVA/UVB stress in the human keratinocyte HaCaT and the wildtype Fibs E6/E7 fibroblast cell lines. The reduction of ROS levels was taken as primary endpoint. The effect of treatment on the cells' metabolic activity was analyzed as an indicator of viability post-treatment to investigate potential immediate and late (photo)toxicity. Additionally, the compounds' antioxidative capacity was investigated using an azo-based radical generator. Established antioxidants, quercetin and N-acetylcysteine, were used as controls. Data showed remarkable differences in the mode of action of the chemical UV filters, ranging from protective to pro-oxidative properties, indicating the need for more detailed mode of action-based investigations. Certainly, additional consideration and evaluation will be necessary to further extrapolate these *in vitro* data for the assessment of *in vivo* exposure situations. However, the presented approach enables parallel investigations of photoprotective and phototoxic effects of UV filters, and thus can complement and extend existing *in vitro* testing strategies.

1 Introduction

The skin as a protective barrier organ is continuously exposed to both chemical and physical insults from the environment, whereby chronic exposure to UV radiation poses a major risk.

UV light that reaches the earth's surface is composed of UVA (320-400 nm) and UVB (280-320 nm). UVC (200-280 nm), and most of the UVB light is already absorbed in the atmospheric ozone layer (de Gruijl et al., 2000). Long-wave UVA radiation can penetrate deep into human skin, reaching the dermis. It is the main reason for photoaging (Bruls et al., 1984; Meinhardt et al., 2008; Krutmann, 2000). Energy-rich UVB radiation is mainly absorbed on the skin's surface and is a major cause of sunburn. UVB exposure can provoke DNA damage directly and contributes to a large extent to photo-carcinogenesis (Bruls et al., 1984; Marionnet et al., 2014).

The increased formation of reactive oxygen species (ROS) is a central process responsible for the negative consequences of UV radiation. The link between UV radiation and skin cancer development is supported by a remarkable number of epidemiological studies (IARC, 1992). According to the World Health Organization (WHO), the global incidences of non-melanoma skin cancers (with 2 to 3 million cases per year) and of melanoma skin cancers (with 132,000 cases per year) have increased up to 5-fold over the past three decades (Leiter et al., 2014; WHO, 2018).

To protect the skin from the detrimental consequences of UV exposure, UV filters are frequently applied that should ideally scatter, reflect, or absorb solar UV radiation and subsequently convert the irradiation energy into harmless energy, like heat, in order to attenuate the damaging effects without the production of radicals (Karsili et al., 2014). Such compounds can be of inorganic nature, for example titanium dioxide (physical UV filters), or are organ-

ic molecules with the ability to absorb light within the UV range (chemical UV filters) (Karsili et al., 2014). In this study, we focused on the chemical UV filter compounds ecamsule, oxybenzone, and menthyl anthranilate.

Oxybenzone, a lipophilic molecule that easily penetrates the skin and may even reach layers beyond the *stratum corneum*, is one of the most widely used UV filters (Sarveiya et al., 2004). It shows intense and broad absorption in the UVA-, UVB-, and UVC-range with absorption maxima at 325 nm, 287 nm, and 243 nm (Baker et al., 2015). Ecamsule is a water-soluble broad-spectrum UVA-absorber with maximum absorbance at 344 nm. This filter is suggested to reduce biological damage caused by solar radiation such as pyrimidine dimer formation, p53 protein accumulation, or collagenase 2 expression (Fourtanier et al., 2008). Menthyl anthranilate is the only liquid UVA sunscreen agent that has been approved by the Food and Drug Administration (FDA) so far, which has facilitated its processing into all kinds of cosmetic formulations. Its UV absorption spectrum shows three maxima at 220 nm, 249 nm, and 340 nm (Beeby and Jones, 2000).

Despite their widespread use, many of these sunscreen compounds are not well characterized concerning their protective capacity against UV-induced ROS stress at a cellular and molecular level. Current standardized testing protocols only cover UV-absorption by cell-free physical measurements (ISO 24443:2012; US FDA, 2018, CFR 21 §327(j)), by grading of erythema formation in humans (sun protection factor, SPF, ISO 24444:2010; US FDA 2018, CFR 21 §352), as well as by measuring of persistent pigment darkening (PPD) to evaluate UVA protection capacities (ISO 24442:2011). However, none of these factors provides detailed information on the ability of the test chemicals to attenuate damaging or potentially mutagenic effects of solar radiation.

Since 2013, animal testing of cosmetic ingredients is banned in Europe due to the prohibition of selling animal-tested cosmetics by the 7th amendment to the EU Cosmetics Regulation (EC, 2009). In addition to ethical and socioeconomic benefits, this was not only a huge trigger for the development and implementation of several *in vitro* methods for testing of chemicals, but also contributed substantially to the reevaluation of cell-culture methods in basic research.

The herein presented *in vitro* model is based on existing testing protocols that were improved in order to be able to screen UV filter compounds for phototoxicity/photoprotection. Such testing systems can serve as a tool to filter out compounds that are not ideal from an efficacy point of view and avoid subsequent ample toxicity testing for these substances, which however may currently also require animal tests, e.g., to assess environmental safety or occupational exposures, as it is the case in Europe. Moreover, although no official guideline-based protocols on photo-irritation and photo-sensitization testing in animals are available, there are protocols from industry, and guidance from the Food and Drug Administration (FDA) and the European Medicines Agency (EMA) is available for pharmaceuticals (SCCS, 2018). Therefore, improving available *in vitro* approaches may support outpacing further development of the *in vivo* approaches.

In this study, we investigated the capacity of the three chemical UV filter compounds ecamsule, oxybenzone, and menthyl anthranilate to influence UVA/UVB stress in the spontaneously immortalized human keratinocyte cell line HaCaT (Boukamp et al., 1988) and the E6/E7 immortalized human wildtype fibroblasts WT Fibs E6/E7 by using the potential intracellular ROS scavenging capacity as endpoint. Oxidative stress was induced by UVA/UVB radiation and by an azo-based radical generator in the absence of UV to differentiate between UV protective capacity and sole ROS scavenging potential. Additionally, the effect of treatment on the cells' metabolic activity was analyzed as an indicator of viability. The established antioxidants quercetin and N-acetylcysteine were used as controls.

There is an urgent need to improve current efficacy testing protocols to better understand the mode of action of these widely used chemicals in order to be able to evaluate their risks and benefits. With the here presented *in vitro* testing system, critical readouts on the mode of action can be generated in a reliable, fast, and cost-effective manner, indicating remarkable differences in the properties of the above-mentioned UV filters.

2 Materials and methods

Chemicals
Oxybenzone (CAS: 131-57-7), menthyl anthranilate (CAS: 134-09-8), and quercetin (CAS: 117-39-5) were dissolved in cell culture grade dimethyl sulfoxide (DMSO); ecamsule (CAS: 92761-26-7) and N-acetylcysteine (CAS: 616-91-1) were dissolved in Hanks' balanced salt solution (HBSS). All chemicals were purchased from Sigma Aldrich (Vienna, Austria). Stocks were prepared freshly before each experiment, except for quercetin stock that was stored at -20°C. IUPAC names of compounds can be found in Table S1[1].

Cell culture maintenance
The spontaneously immortalized human keratinocyte cell line HaCaT (Boukamp et al., 1988) (Cell Lines Service, Eppelheim, Germany) was cultured in Roswell Park Memorial Institute's medium (RPMI, Sigma Aldrich, Austria) supplemented with 10% (v/v) fetal bovine serum (FBS, Life Technologies, Darmstadt, Germany). E6/E7 immortalized human wildtype fibroblasts (WT Fibs E6/E7) were kindly provided by EB House Austria, Department of Dermatology, University Hospital Salzburg of Paracelsus, Private Medical University Salzburg, Austria. WT Fibs E6/E7 cell lines were generated from skin tissue removed in the course of a routine surgery (breast reduction) upon written informed consent obtained from the patient in accordance with the Declaration of Helsinki and the applicable national, institutional and data protection laws. They were maintained in low glucose Dulbecco's Modified Eagle Medium (DMEM, Sigma Aldrich, Austria) supplemented with 10% (v/v) FBS. Both cell lines were cultured in a humidified atmosphere containing 5% (v/v) CO_2 at 37°C. No antibiotics or antimycotics were used.

Experimental dose selection

UV filters in sunscreens can be present in concentrations up to several hundred millimoles per liter. The UV filters investigated in this study were approved by the US FDA or Health Canada or the European Commission with maximum allowed concentrations up to 6% for oxybenzone, up to 5% for menthyl anthranilate, and up to 10% for ecamsule (US FDA, 2018, CFR 21 § 352; Health Canada 2012; EC, 2009). Though data on the bioavailability is available, this is not sufficient to draw final conclusions on the real exposure concentrations in layers beyond the *stratum corneum*, because several factors such as applied dose, penetration capacity, metabolism, hydrophilicity, etc. have to be considered. Best studied is oxybenzone, for which human plasma concentrations (free form) in the very low micromolar range were found after topical application of oxybenzone containing sunscreen in a study with a very limited number of participants (n = 3). The determination of the excreted compound and its metabolites pointed towards high systemic absorption and fast metabolism (Sarveiya et al., 2004). Calafat et al. (2008) determined urine concentrations (free and conjugated forms) in human volunteers without prior envisaged treatment, reporting concentrations in the low micromolar range (n = 2517). Dermal penetration of ecamsule was suggested to be less than 0.1% of experimentally applied doses, and ecamsule and metabolites could be detected in urine (n = 5 participants) (Benech-Kieffer et al., 2003). Only little information is available for menthyl anthranilate.

The *in vitro* testing concentrations for the UV filter compounds were adapted according to the maximum allowed doses, considering (potential) dermal penetration, hydrophilicity (solubility in the testing buffer), and effects on cell viability. The cells were treated either with increasing concentrations of ecamsule or oxybenzone ranging from 200 to 1600 µM or menthyl anthranilate ranging from 25 to 100 µM. Ecamsule was dissolved in HBSS; the pH had to be adjusted to 7.0 by adding 0.1 N sodium hydroxide (approximately 2 µl/ml). In commercially available sunscreen formulations, ecamsule is used as a salt after neutralization (Fourtanier et al., 2008). The DMSO-dissolved stock solutions of menthyl anthranilate and oxybenzone were further diluted in HBSS, mixed on a vortex shaker, sonicated for 5 min at room temperature, and incubated for 15 min at 37°C, 800 rpm. The vehicle control (DMSO) concentrations were chosen according to the highest concentration applied with the respective test substance (max. 1% for fibroblasts and max. 2% (v/v) for keratinocytes DMSO in HBSS). The antioxidants quercetin at 10 and 20 µM final concentration and N-acetylcysteine at 800 and 1600 µM were applied as positive controls.

Determination of intracellular antioxidant activity

Cell suspensions containing either 5×10^4 HaCaT cells/100 µl or 2×10^4 WT Fibs E6/E7 cells/100 µl were seeded in a 96-well plate. HaCaT were incubated for 24 h and WT Fibs E6/E7 for 65 h to reach confluency. Treatment duration with the UV filter compounds was 1 h. Untreated cells were used as control. For one substance, all exposures, treatments, and controls were performed in parallel using one single 96-well plate. At least three independent experiments were performed with each compound.

To measure the relative changes of intracellular ROS activity, the fluorescent probe 2',7'-dichlorofluorescin diacetate (DCFH-DA) (Sigma Aldrich, Vienna, Austria) was used as substrate, based on the original protocol of Wolfe and Liu (2007), with several modifications. Confluent cells were washed twice with prewarmed phosphate buffered saline (PBS), followed by a treatment with 50 µl per well of 25 µM DCFH-DA in HBSS. DCFH-DA passes through the cell membranes and it is subsequently deacetylated by intracellular esterases to DCFH, which is trapped within the cell. In the presence of ROS, DCFH rapidly oxidizes to its highly fluorescent derivative 2'-7'-dichlorofluorescein (DCF). The intensity of the fluorescence signal is proportional to the level of intracellular ROS. Together with the DCFH-DA treatment, cells received 50 µl of test solution, buffer, or solvent controls for 1 h at 37°C.

After washing with PBS, the 96-well plate was divided into 3 sections: to one section 600 µM of the peroxyl radical generator 2-[(1-amino-1-imino-2-methylpropan-2-yl)diazenyl]-2-methylpropanimidamide (AAPH) (Sigma Aldrich, Vienna, Austria) in HBSS was added, the second section was treated with UV radiation (312 nm, details are described below), and the third section was left untreated. After 45 min of incubation at 37°C in the dark, the fluorescence of DCF was determined (excitation 485 nm/ emission 538 nm) using a Tecan infinite F200 PRO plate reader (Tecan Group Ltd., Männedorf, Switzerland).

UV exposure

Cells were exposed to UV radiation using an Ultraviolet Transilluminator Unit 312 nm (Intas UV-Systeme, Göttingen, Germany), which emits 4.91 mJ/cm²/s of UVA irradiation and 0.38 mJ/cm²/s in the Erythema Action Spectrum (EAS). Irradiation doses were determined using the Datalogging Radiometer Solar® Light (Glenside, USA) equipped with suitable UVA- and erythema weighted sunburning-UV-(SUV)-detectors. The former covers the range of 320 nm to 400 nm; the spectral response of the SUV-detector closely follows the EAS, which lies in the UVB range.

Determination of cell viability

The metabolic conversion of resazurin to resorufin was used as a measure for viability, which was estimated 1 h and 24 h post-treatment with AAPH and UV radiation, respectively. After washing with PBS, 100 µl growth medium including 10% (v/v) of Cell-Titer-Blue reagent (Promega, Mannheim, Germany) was added to the cells. Cells were incubated for 50 min (for HaCaT cells) or 75 min (for WT Fibs E6/E7 cells) at 37°C in the dark. The formation of resorufin was determined at 560 nm excitation/590 nm emission (Tecan infinite F200 PRO plate).

Live cell imaging

Images of the cells were taken 24 h post-treatment. Growth medium containing wheat germ agglutinin (WGA, Alexa Fluor 647 conjugate) (5 µg/ml, Molecular Probes, Invitrogen, Paisley, UK), Hoechst 33342 stain (0.5 µg/ml; Sigma Aldrich, Vienna, Austria), and propidium iodide (500 nM; Molecular Probes, Invitrogen, Paisley, UK) were added to the cells for 20 min at room temperature. WGA binds to sialic acid and N-acetylglucosaminyl residues on the plasma membrane. Hoechst 33342 is a cell-perme-

able DNA stain, while propidium iodide cannot penetrate intact cell membranes and indicates apoptotic and dead cells. Real-time live confocal imaging was performed with a spinning disc confocal system (UltraVIEW VoX; Perkin Elmer, Waltham, USA) connected to a Zeiss AxioObserver Z1 microscope (Zeiss, Oberkochen, Germany). Images were acquired with the Volocity software (Perkin Elmer) using a 10x and 40x water immersion objective.

Statistical analysis
For statistical analysis, the IBM SPSS Statistics Software version 25 (Armonk, USA: IBM Corp.) was used. Non-parametric testing was performed, as not all data showed normal distribution, using Friedman, Wilcoxon signed-rank, Kruskal-Wallis and Mann–Whitney U

tests. Differences were considered to be of significance if $p \leq 0.05$. The half maximal inhibitory concentration (IC_{50}) for the UV filters was assessed using the CalcuSyn software version 1.1.1 (Biosoft, Cambridge, UK), according to the concept of Chou and Talalay (1984). IC_{50} values of quercetin and N-acetylcysteine were calculated by linear regression due to the availability of only 2 data points.

3 Results

3.1 Optimization of UV exposure conditions
The experimental setup was optimized by exposing the keratinocyte cell line HaCaT to 4.91 mJ/cm²/sec UVA/0.38 mJ/cm²/sec
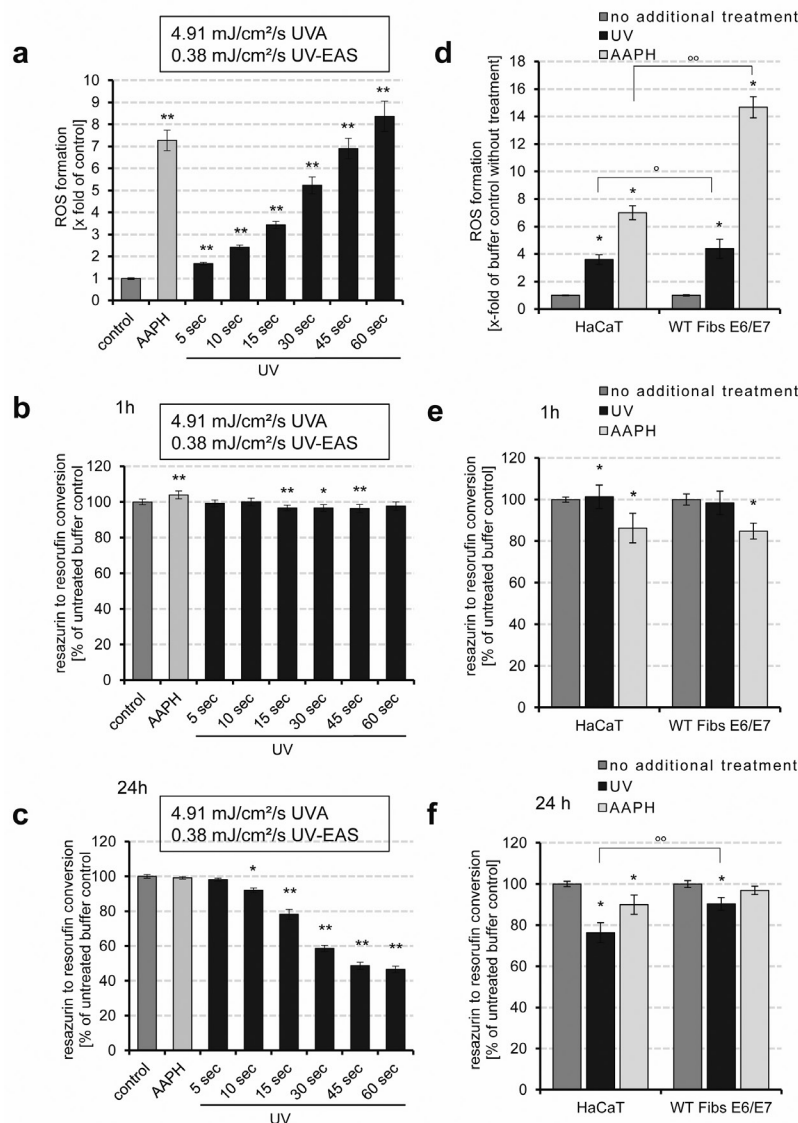

Fig. 1: Optimization of UV exposure conditions
(a) ROS formation in HaCaT cells exposed to UV radiation for up to 60 sec, or to 600 μM AAPH as positive control was compared to buffer-treated control cells (set to 1). The impact of UV exposure and AAPH-treatment on the conversion of resazurin, an indicator of cell viability, was assessed in HaCaTs at 1 h (b) and 24 h (c) post-treatment compared to buffer treated cells (set to 100%). The effects of 15 sec UV exposure and AAPH treatment is shown for HaCaT and WT Fibs E6/E7 cells, with regard to ROS formation (d) and cell viability at 1 h (e) and 24 h (f) post-treatment. Significant differences in comparison to the respective untreated controls are indicated with an asterisk (*) and circles (°) indicate differences between the cell types. Results shown are means ± SEM of at least 3 independent experiments, each performed at least in triplicates (*p ≤ 0.05, **p ≤ 0.005 compared to the respective control).

UV EAS for increasing time intervals. ROS formation and the metabolic activity, an indicator of cell viability, were used as read-out. The optimal exposure time was considered as the treatment period after which ROS-formation occurred but viability was affected only to a minor extent. Treatment with the peroxyl radical generator AAPH was used as positive control.

As indicated in Figure 1a, ROS-formation increased in a time-dependent manner, reaching an 8.4-fold increase compared to baseline after 60 sec. After 45 sec exposure time, the DCF fluorescence was comparable to the effect induced by 600 µM AAPH. The treatment duration of 15 sec was considered optimal, resulting in a dose of 73.65 mJ/cm² UVA and 5.70 mJ/cm² UV EAS, after which oxidative stress levels were 3.3-fold increased. One hour

after exposure, the metabolic activity was not impaired (Fig. 1b), while a dose-dependent reduction was observed 24 h post-treatment (Fig. 1c). The 15 sec exposure reduced the viability by 22% compared to the untreated control.

The same UV exposure conditions were investigated for the WT Fibs E6/E7 fibroblast cells (Fig. 1d-f). DCF fluorescence levels were 4.4-fold elevated after a 15 sec treatment with UV-light and 14.7-fold increased due to the AAPH-treatment, compared to untreated cells. One hour post-treatment, metabolic activity of those cells that had been treated with AAPH was impaired by 15.2% compared to controls, but there was no reduction due to UV exposure. The damaging effects of irradiation could be witnessed 24 h later, when metabolic activity decreased by 9.7% compared to the control.
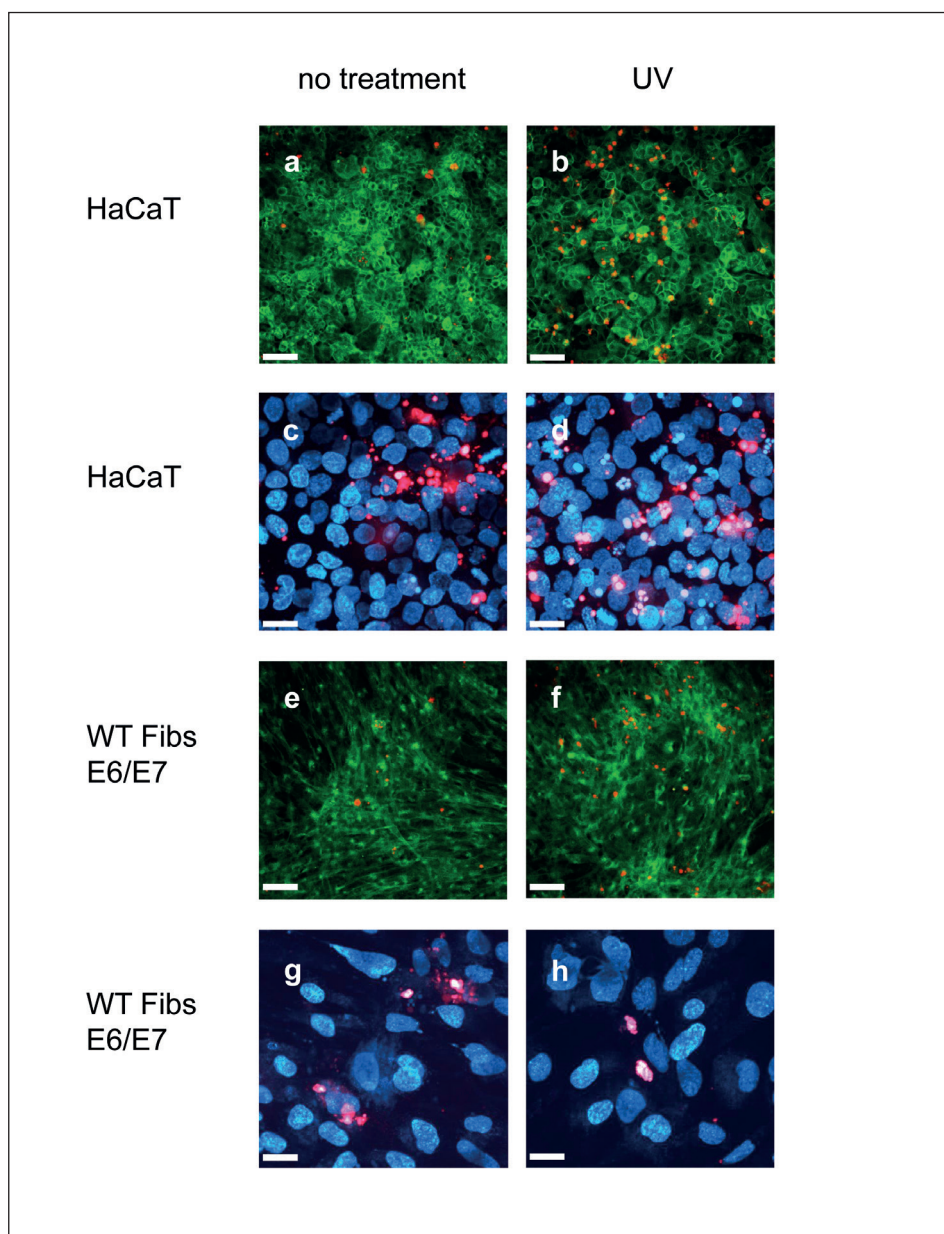

Fig. 2: Real time live confocal analysis of HaCaT keratinocytes (a-d) and WT Fibs E6/E7 fibroblasts (e-h)
The cells were either left untreated (a,c,e,g), or were exposed to UV radiation (b,d,f,h). After a recovery period of 24 h, cells were stained with wheat germ agglutinin (green), Hoechst 33342 (blue), and propidium iodide (red) to investigate cell viability and morphology. Scale bar: 20 µM (c,d,g,h); scale bar: 80 µM (a,b,e,f).

While the differences in susceptibility towards UV irradiation between the two cell types was only minor though significant (p = 0.043), the WT Fibs E6/E7 were much more sensitive to treatment with the radical generator AAPH compared to HaCaT cells, e.g., ROS-formation induced by 600 µM AAPH was 2.1-fold higher in WT Fibs E6/E7 than in HaCaTs (p < 0.001).

In addition, microscopic analysis was used to investigate changes in cell viability and morphology affected by a 15 sec UV exposure (Fig. 2a-d). UV exposed HaCaT cells exhibited fewer cell-cell contacts and significantly more apoptotic cells 24 h post-treatment compared to the untreated keratinocytes. In both conditions, the majority of the cells were viable, and the presence of several metaphases indicated active cell division. While in the untreated samples the few cells undergoing apoptosis were located in close proximity, the apoptotic cells were found to be evenly distributed over the investigated culture areas in the irradiated sample. In the untreated WT Fibs E6/E7 sample, the number of apoptotic/dead cells was slightly but not significantly lower compared to the untreated keratinocytes (8.6 ± 3.0% compared to 10.6 ± 4.4% in keratinocytes, p = 0.456). Likewise, the effect of UV irradiation was not significantly different (17.1 ± 4.8% in fibroblasts compared to 20.2 ± 6.2% in keratinocytes, p = 0.351) (Fig. 2e-h).

3.2 Effect of antioxidant compounds

The cells were treated with the well-known antioxidant controls quercetin and N-acetylcysteine (Fig. 3a) (Nimse and Pal, 2015; Rushworth and Megson, 2014) in parallel under baseline conditions and in the presence of ROS, triggered either by UV irradiation or by chemical induction.

Quercetin significantly and dose-dependently inhibited ROS-formation in both AAPH- and in the UV treated HaCaT and WT Fibs E6/E7 cells (Fig. 4a,b). In addition, physiological (baseline) ROS levels were reduced by approximately 52.3% in HaCaT and 55.7% in WT Fibs E6/E7 upon treatment with 20 µM quercetin. Under the selected exposure conditions and when normalized to the respective controls, quercetin mediated protection against ROS stress was strongest for AAPH-induced stress, followed by reduction of physiological ROS levels, while it was less protective against UV induced stress. Half maximal inhibitory concentrations (IC_{50}) of 68.39 µM for HaCaT and 65.82 µM for WT Fibs E6/E7 were reached in the UV irradiation setting, compared to 9.18 µM (HaCaT) and 10.00 µM (WT Fibs E6/E7) for the AAPH-treatment.

N-acetylcysteine showed weaker antioxidant capacities compared to quercetin and was therefore applied at higher concentrations (Fig. 4c,d). Its protective capacity was strongest for the chemically-induced ROS stress, followed by the reduction of physiological ROS levels, under the selected conditions and compared to the respective controls. IC_{50} values of 1692 µM in HaCaT and of 514 µM in WT Fibs E6/E7 were determined in the AAPH exposure setting. No interference with UV induced ROS was observed at the selected concentrations.

Some effects on cell viability of quercetin and N-acetylcysteine treatment (in addition to the UV or AAPH treatment effects) leading to a maximum reduction of 10.3 ± 4.0% (mean ± S.E.M.) were observed both after 1 and 24 h post treatment (Fig. S1 and
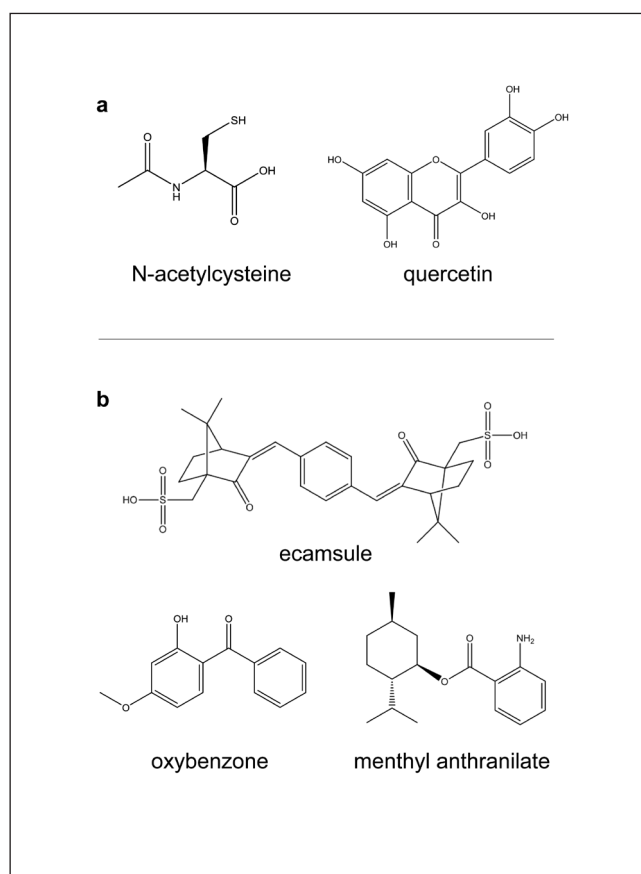
Fig. 3: Chemical structures of the tested antioxidants N-acetylcysteine and quercetin (a), and of the chemical UV filters ecamsule, oxybenzone, and menthyl anthranilate (b)

S2[1]). All IC_{50} values including upper and lower confidence intervals are given in Tables S2, S3, and S4[1].

3.3 Effect of the UV filter compounds

The three widely used chemical UV filters oxybenzone, menthyl anthranilate, and ecamsule (see Fig. 3b) were tested for their capacities to counteract UV and AAPH induced ROS.

Oxybenzone, a broad-spectrum sunscreen, significantly decreased UV induced oxidative stress in HaCaT cells at the highest test concentration of 1600 µM compared to the vehicle control (DMSO) (Fig. 5a). At this concentration, a reduction of 29.0% in relation to the HBSS control and of 18.0% compared to the vehicle control could be observed. Of note, also the vehicle DMSO had some effect at the concentration that had to be used in these experiments (2% (v/v)). Baseline ROS-levels were also significantly decreased with 1600 µM oxybenzone compared to vehicle control, while no such effect was observed in the AAPH setting compared to the respective vehicle control.

Viability measured after 1 h was attenuated by 8.0% with the highest concentration of oxybenzone applied prior to UV irradiation and a reduction of viability by 11.9% compared to the vehicle control was seen if the sunscreen agent was applied without additional treatment (Fig. 5b). The co-exposure of AAPH and

oxybenzone did not result in significant changes in viability after 1 h. No oxybenzone-mediated reduction of cell viability could be observed at 24 h post-treatment in all three settings (Fig. S3c[1]).

Oxybenzone demonstrated stronger UV-protective and antioxidative activity in WT Fibs E6/E7 compared to the HaCaT cells (Fig. 5c). It decreased ROS formation dose-dependently, at concentrations ranging from 200 µM to 800 µM in all three test settings. Cells treated with 800 µM oxybenzone reached a decrease in ROS level of 34.3% upon UV radiation, by 25.7% following AAPH-treatment, and by 34.2% at baseline conditions compared to the respective vehicle controls. Some reducing effect of the vehicle (1% (v/v) DMSO) on ROS levels was observed (up to 12.1% reduction compared to the buffer controls). Higher concentrations of oxybenzone were not tested in this cell model to reduce the impact of the vehicle, as effects were already present at 800 µM.
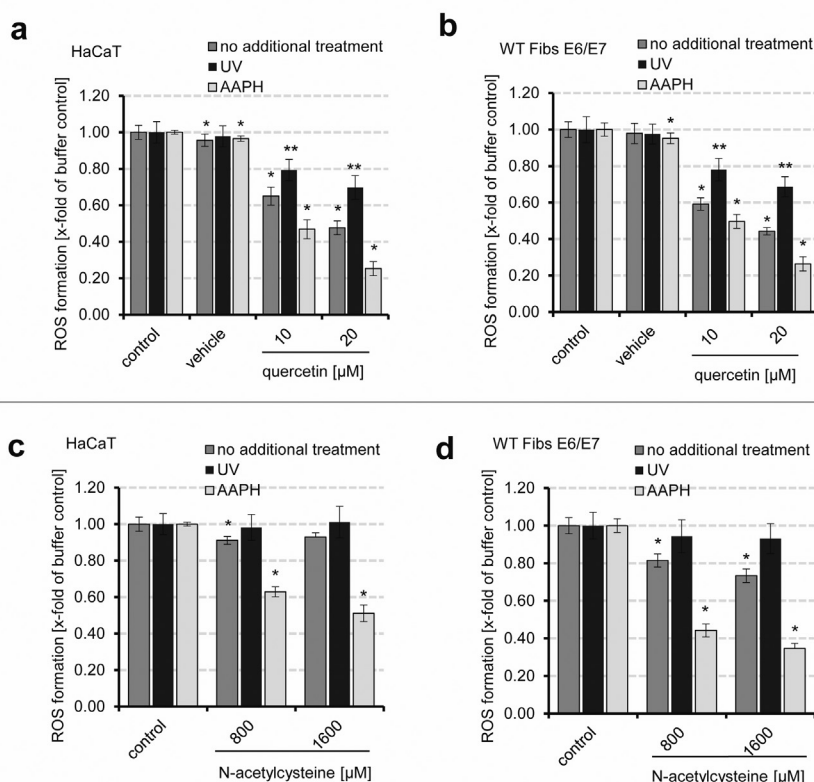
The cell viability decreased slightly but significantly under baseline and UV treated conditions with increasing concentrations of oxybenzone, compared to the vehicle control, 1 h after the treatment (Fig. 5d). For the highest concentration of oxy-

benzone, a decrease in viability remained even 24 h post-treatment. At this time point, also AAPH-treated cells were affected (Fig. S3f[1]). Viability was reduced by approximately 4-9% for all treatments, compared to the vehicle controls.

Menthyl anthranilate, an organic UVA filter, displayed both pro- and antioxidant properties. In HaCaT keratinocytes treated with the compound, UV induced ROS-formation increased significantly over the whole concentration range from 25 to 100 µM, with an increase by 19.2% at the highest concentration compared to the buffer control (Fig. 6a). Less pronounced pro-oxidant effects were observed in the cells receiving no additional treatment and upon AAPH-stimulation with a maximum augmentation of 8.1% (no treatment) and 10.2% (AAPH) compared to the respective buffer controls. The UV exposed cells displayed a minor reduction of cell viability 1 h after the treatment at the higher test concentrations (50 and 100 µM) (Fig. S4b[1]). 24 h after treatment, cell viabilities were indirectly proportional to the sun filter's concentrations. In the cells receiving 100 µM menthyl anthranilate, the resazurin conversion was reduced by 10.8% with no additional treatment, by 11.2% if AAPH-treatment was

Fig. 4: Impact of quercetin (a,b) and N-acetylcysteine (c,d) on intracellular ROS levels, in HaCaT keratinocyte and WT Fibs E6/E7 fibroblast cells

For better comparison, the effect on ROS formation is shown in relation to the respective compound's untreated control of each setting (set to 1). UV and AAPH exposure settings led to an increase of ROS-levels by 4.01 ± 0.28-fold and 6.12 ± 0.67-fold in HaCaT, and by 4.75 ± 0.68-fold and 14.89 ± 1.0-fold in WT Fibs E6/E7 cells, compared to baseline (= without compound addition and compared to the untreated controls). The maximum vehicle concentration was 0.08% (v/v) DMSO for quercetin; N-acetylcysteine was dissolved in buffer only. Results show means ± SEM of 3 independent experiments, each performed at least in triplicates (*p ≤ 0.05, **p ≤ 0.005 compared to the respective control).

applied and by 14.3% in the UV treated cells, in comparison to the respective buffer controls (Fig. 6b). Some effect of the vehicle (0.25% (v/v) DMSO) on viability was observed in the otherwise untreated cells (maximal 8% for viability reduction after 1 h).

Fibroblasts generally displayed a higher susceptibility towards menthyl anthranilate super-induction of UV-stress compared to the keratinocytes (Fig. 6c). Upon UV exposure, a maximum increase in ROS-formation by 11.2% was observed at the treatment concentration of 25 µM (compared to the buffer control). ROS levels remained elevated at higher treatment concentrations but showed no dose-dependency. On the contrary, AAPH-induced and baseline ROS formation were quenched by the compound in a dose-dependent manner with a significant attenuation of oxidative stress compared to buffer-treated control cells. Incubation with 100 µM menthyl anthranilate led to a reduction of 23.6% for the AAPH-treatment setting and of 25.4% without additional treatment. In this cell type also the vehicle (0.25% (v/v) DMSO) led to some reduction of ROS (up to 10.8%) and viability (up to 11.5% after 1 h), compared to the respective buffer con-

trols. Cells receiving no additional treatment were most sensitive towards DMSO.

For all exposure conditions, the viability decreased in a dose-dependent manner one day after the treatment (Fig. 6d, Fig S4e,f[1]). Cells showed a 34.3% decline in the metabolic activity compared to buffer control if pre-treated with 100 µM menthyl anthranilate prior to UV exposure. The sunscreen agent displayed lower cytotoxic activity in AAPH-treated and untreated cells with maximum declines in cell viability of 30.5% (AAPH) and 19.9% (no treatment), respectively.

Treatment of HaCaT cells with the UVA filter ecamsule in the concentration range of 200 to 1600 µM resulted in only minor effects. UV induced oxidative stress was reduced by 14.5% upon 1600 µM treatment compared to the respective control (Fig. 7a). When no ROS-inducing treatment was performed, ecamsule exhibited a non-monotonic dose-response by increasing basal ROS levels at treatment concentrations up to 800µM with a maximum increase of 12.6% at a concentration of 200 µM, while 1600 µM ecamsule did not provoke significant changes. No significant ef-
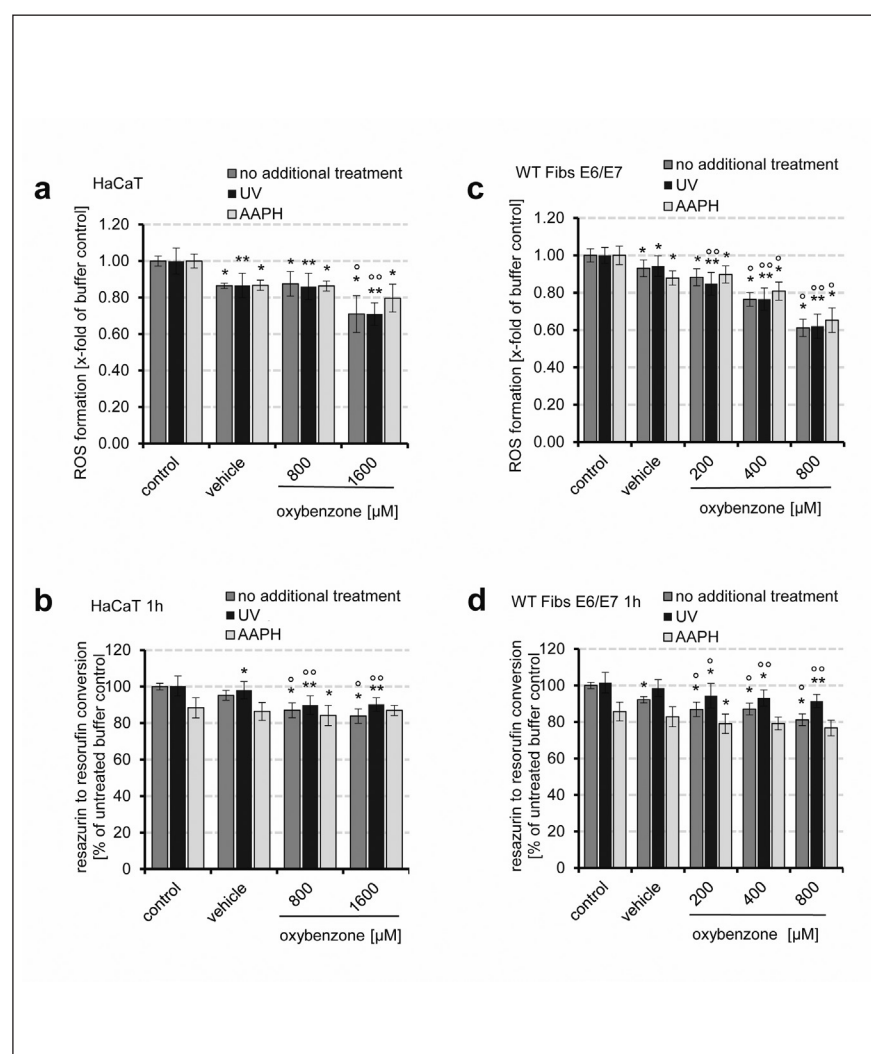

Fig. 5: Impact of increasing concentrations of oxybenzone on intracellular ROS formation in (a) HaCat and (c) WT Fibs E6/E7 cells exposed to UV, AAPH, or without additional treatment
The effect on ROS formation is shown in relation to the respective untreated control of each setting (set to 1). UV and AAPH exposure settings led to an increase of ROS-levels by 3.58 ± 0.28-fold and 7.28 ± 0.47-fold in HaCaT, and by 4.56 ± 0.85-fold and 16.04 ± 1.03-fold in WT Fibs E6/E7 cells, compared to baseline (= without compound addition and compared to the untreated controls). Effects on cell viability estimated by resazurin conversion in HaCaT and on WT Fibs E6/E7 cells 1 h post-treatment (b,d). Results were normalized to the respective buffer controls (set to 100%). 24 h post-treatment there were no effects on cell viability in HaCaT cells, effects in Fibs E6/E7 were less pronounced (Fig. S3[1]). Vehicle concentrations of 2% (v/v) DMSO (for HaCaT) and 1% (v/v) (for WT Fibs E6/E7) were used. Results are shown as mean values ± S.E.M. of 3 independent experiments, each performed at least in triplicates (*p ≤ 0.05, **p ≤ 0.005 compared to control, °p ≤ 0.05, °°p ≤ 0.005 compared to vehicle).

fect of ecamsule was detected in the AAPH-setting. Minor but significant cell viability impairing effects could be observed 1 h later in the cells receiving no additional treatment with a maximum of 12.6% reduction at an ecamsule concentration of 1600 µM, compared to the respective control (Fig. 7b). No effects on cell viability were observed for the compound treatment in all three settings 24 h post-treatment.

WT Fibs E6/E7 cells were more sensitive towards ecamsule treatment. In the fibroblasts, the compound counteracted UV and AAPH induced ROS-formation. In addition, basal ROS levels were reduced. The effects were dose-dependent, reaching a maximum ROS reduction by 25.7% at the highest tested concentration of 1600 µM in the UV-setting. With the same concentration of ecamsule, oxidative stress that had been trigged by AAPH was reduced by 10.8% and basal levels were attenuated by 16.9%, compared to the respective controls. A significant but weak reduction of cell viability (approximately 8%) was observed to the UV exposure setting over the whole concentration range, while ecamsule increased the viability at the highest applied concen-

tration of 1600 µM in the AAPH-treated cells (Fig. 7d). At the later time point, cells did not show an impairment of viability for most of the treatment concentrations and conditions (Fig. S5f).
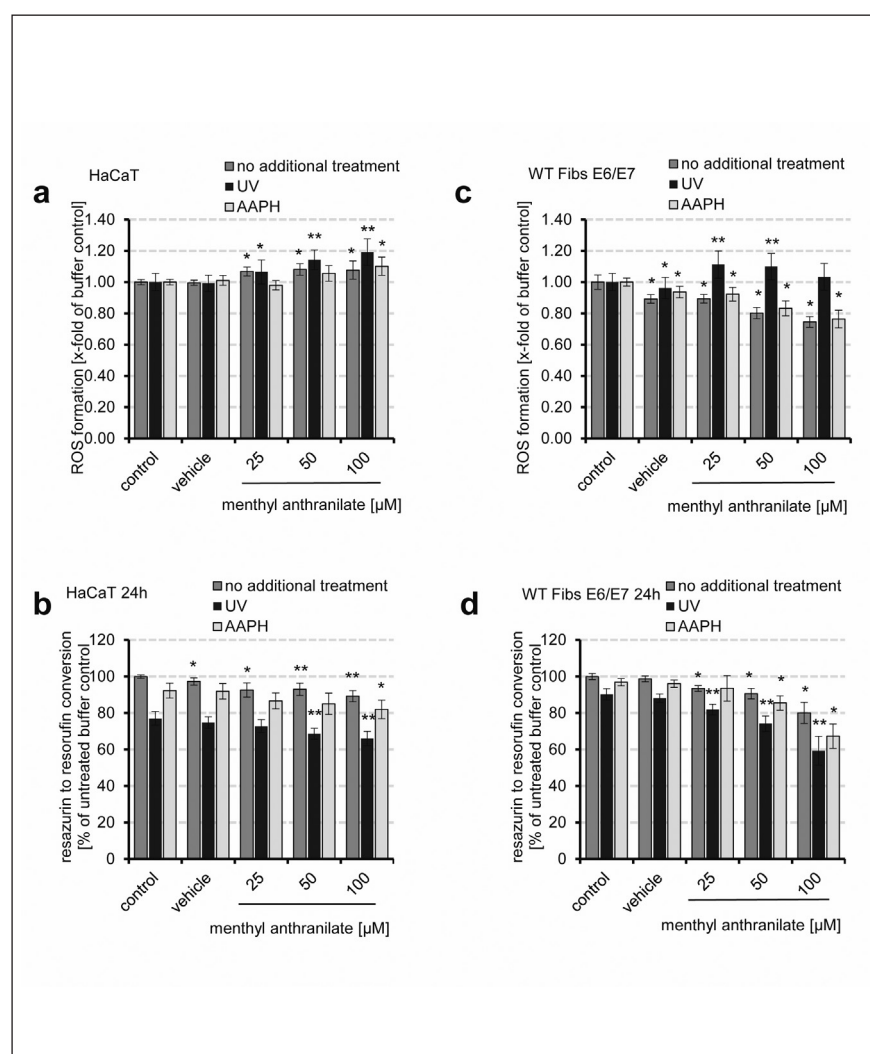
A summary of all maximal effects for each compound, experimental setting, and cell line can be found in Table 1.

4 Discussion

Increased exposure to UVA/B irradiation leads to the formation of oxygen radicals including singlet oxygen in the skin. The application of organic UV filters is intended to protect the skin from the resulting oxidative stress by absorbing light in the UV spectrum leading to electronic excitation of the molecule. Ideally, this excitation should be exclusively transformed into vibrational energy and subsequently dissipate as heat (Karsili et al., 2014). If a compound only absorbs UV light but does not have the capacity to convert the energy into less harmful forms, radicals will be produced, and oxidative stress can arise. Therefore,

Fig. 6: Impact of menthyl anthranilate on intracellular ROS formation in (a) HaCat and (c) WT Fibs E6/E7 cells exposed to UV, AAPH or without additional treatment

For better comparison, the effect on ROS formation is shown in relation to the respective untreated control of each setting (set to 1). UV and AAPH exposure settings led to an increase of ROS-levels by 3.68 ± 0.30-fold and 6.42 ± 0.65-fold in HaCaT, and by 4.38 ± 0.69-fold and 14.67 ± 0.76-fold in WT Fibs E6/E7 cells, compared to baseline (= without compound addition and compared to the untreated controls). Effect of menthyl anthranilate on HaCaT and on WT Fibs E6/E7 viability at 24 h post-treatment (b,d) were more pronounced than at 1 h post-treatment (Fig. S4[1]). Cell viability is shown in comparison to the unstimulated buffer control (set to 100%). DMSO was used with 0.25% (v/v) as vehicle in both cell lines. Results are shown as mean values ± S.E.M. of at least 3 independent experiments, each performed at least in triplicates (*p ≤ 0.05, **p ≤ 0.005 compared to control, °p ≤ 0.05, °°p ≤ 0.005 compared to vehicle).

investigations on the properties of sunscreen compounds are of major importance.

The herein described assay aims to screen for compounds with potential photoprotective capacities in a routine testing setting, in analogy to the OECD TG 432 for phototoxic compounds, but amended by the use of human cell lines and by additionally focusing on oxidative stress as readout, in line with a suggestion from SCCS (2018). OECD TG 432 is based on the uptake of neutral red to estimate the viability of murine embryonal fibroblasts (3T3) after irradiation (OECD, 2004) as only parameter. Both the neutral red uptake and the resazurin reduction assay are commonly used cell enumeration assays, whereby the latter is not cytotoxic so that follow-up experiments in the same cells can be performed (van Tonder et al., 2015).

The study profited from work of several groups that previously developed and improved similar assays based on, e.g., microscopy, flow-cytometry, but also fluorescence measured in plate-formats, in terms of cost- and time-effectiveness, and throughput (Armeni et al., 2004; Wolfe and Liu, 2007; Ryu et al., 2014; Klein et al., 2013). Though some of these studies also used irradiated

cells, the here proposed test setting is advantageous due to the parallel estimate of a test compound's dose-dependent activity under three different conditions (no treatment, controlled UVA/UVB exposure, and AAPH treatment) on one culture plate, and by using two different readouts (oxidative stress and immediate and delayed reduction of cell viability). This allows a comparison of effects among different experiments and also among different substances by referring to the control conditions that are present on each assay plate (e.g., untreated, UV treated). In addition, the exposure conditions can be adjusted if testing on other cell types or use of specific UV wavelengths or solar simulators is required. This study focused on the evaluation of ROS scavenging capacities of the three commonly used sunscreen ingredients oxybenzone, menthyl anthranilate, and ecamsule following UV exposure.

Quercetin was selected as positive control as it is a well-studied phytochemical belonging to the family of flavonoids, which are known for their broad antioxidative properties (Nimse and Pal, 2015). In the plant kingdom, the UV protective capacity of quercetin is well established: When plants are exposed to UV irradiation, their content in especially quercetin increases. Thus,
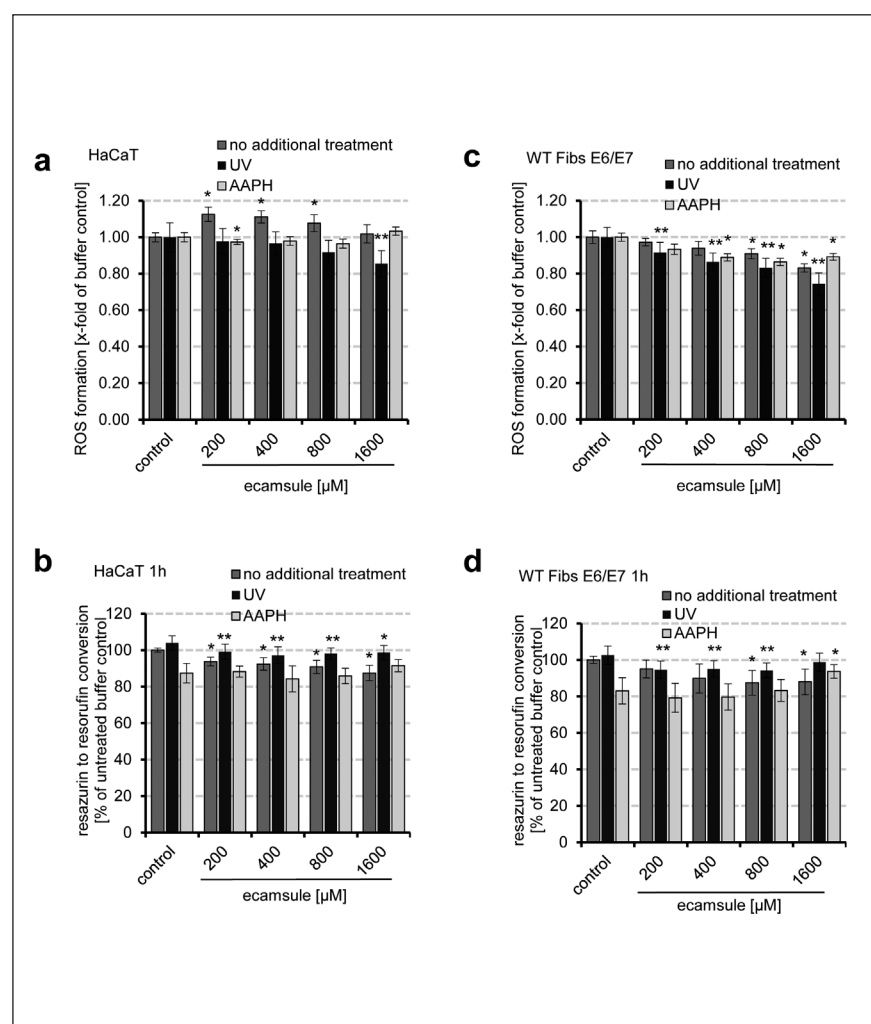

Fig. 7: Impact of increasing concentrations of ecamsule on ROS levels in (a) HaCat and (c) WT Fibs E6/E7 cells after UV exposure, AAPH-treatment or without additional treatment

The effect on ROS formation is shown in relation to the respective untreated control of each setting (set to 1). UV and AAPH exposure settings led to an increase of ROS-levels by 3.94 ± 0.34-fold and 5.79 ± 0.17 fold in HaCaT, and by 5.49 ± 0.34-fold and 15.93 ± 0.58-fold in WT Fibs E6/E7 cells, compared to baseline (= without compound addition and compared to the untreated controls). Effects of ecamsule on cell viability of HaCaT and WT Fibs E6/E7 at 1 h post-treatment (b,d). After 24 h only minor effects on cell viability fo WT Fibs E6/E7 were found (Fig. S5[1]). Viability data were normalized to the unstimulated buffer control (set to 100%). Results are shown as mean values ± S.E.M. of 3 independent experiments, each performed at minimum in triplicates (*p ≤ 0.05, **p ≤ 0.005 compared to control, °p ≤ 0.05, °°p ≤ 0.005 compared to vehicle).

Tab. 1: Summarizing table showing the maximum effects of compounds on ROS levels as well as on cell viability measured 1 h or 24 h post-treatment in HaCaT and WT Fibs E6/E7 cells after UV exposure, AAPH-treatment, or without additional treatment, compared to the respective baseline controls (set to 100%; for oxybenzone the vehicle control was used for comparison)
The table includes all significant effects ≥ | 5% | (p ≤ 0.05). Asterisks indicate compounds for which non-monotonic responses were observed; no treat., no treatment.

Substance	Cell type	Setting	[%] Maximum decrease/increase of ROS	[%] Change in cell viability (1 h post-treatment)	[%] Change in cell viability (24 h post-treatment)	Maximum effect observed with a treatment concentration of x [μM]
quercetin	HaCaT	no treat.	-52.3	-8.7	n.s.	20
		UV	-30.2	n.s.	n.s.	20
		AAPH	-74.7	n.s.	n.s.	20
	WT Fibs E6/E7	no treat.	-55.7	-10.3	n.s.	20
		UV	-31.3	-6.9	-9.4	20
		AAPH	-73.6	n.s.	n.s.	20
N-acetylcysteine	HaCaT	no treat.	-8.9	-6.7	n.s.	800
		UV	n.s.	n.s.	-5.2	800
		AAPH	-48.9	n.s.	n.s.	1600
	WT Fibs E6/E7	no treat.	-26.7	-9.8	-5.3	1600 (ROS, viab 24h) / 800 (viab 1h)
		UV	n.s.	-6	-8	800
		AAPH	-65.4	n.s.	n.s.	1600
oxybenzone	HaCaT	no treat.	-17.9	-11.9	n.s.	1600
		UV	-18	-8.3	n.s.	1600 (ROS) / 800 (viab)
		AAPH	-8.2	n.s.	n.s.	1600
	WT Fibs E6/E7	no treat.	-34.2	-11.9	-8.5	800
		UV	-34.3	-7.2	n.s.	800
		AAPH	-25.7	n.s.	-8.2	800
menthyl anthranilate	HaCaT	no treat.	8.1	-10	-10.8	50 (ROS) / 100 (viab)
		UV	19.2	-7.1	-14.3	100 (ROS, viab 24h) / 50 (viab 1h)
		AAPH	10.2	n.s.	-11.2	100
	WT Fibs E6/E7	no treat.	-25.4	n.s.	-19.9	100
		UV	11.2 *	-9.3	-34.3	25 (ROS) / 50 (viab 1h) / 100 (viab 24h)
		AAPH	-23.6	n.s.	-30.5	100
ecamsule	HaCaT	no treat.	12.6 *	-12.6	n.s.	200 (ROS) / 1600 (viab)
		UV	-14.5	-6.5	n.s.	1600 (ROS) / 400 (viab)
		AAPH	n.s.	n.s.	n.s.	-
	WT Fibs E6/E7	no treat.	-16.9	-12.5	n.s.	1600 (ROS) / 800 (viab)
		UV	-25.7	-8.1	n.s.	1600 (ROS) / 800 (viab)
		AAPH	-10.8	12.8	n.s.	1600

plants containing higher amounts of quercetin can better cope with UVB light (Ryan et al., 2008). Although being one of the most investigated, the photoprotective effect of quercetin in human cells was reported only a few years ago (Maini et al., 2015). In the present study, quercetin reduced radical formation significantly under all investigated experimental conditions: upon UV exposure and AAPH-stimulation, as well as under basal conditions, with IC_{50} values in the micromolar range. The effects were similar in both cell types, keratinocytes as well as fibroblasts. N-acetylcysteine, which was chosen as a second control, is a prodrug that leads to the synthesis of the powerful detoxifying agent glutathione (Rushworth and Megson, 2014). It demonstrated antioxidant activities under AAPH- and basal conditions, but did not exhibit protective effects from oxidative stress induced by UV radiation. This result indicates that not every antioxidant inhibits UV induced ROS-formation.

Oxybenzone is a commonly used broad spectrum organic UV filter absorbing both UVA and UVB light. It is readily absorbed after dermal application (Sarveiya et al., 2004). In rats, the compound itself and three of its phase-I metabolites (2,4-dihydroxybenzophenone (DHB), 2,2′-dihydroxy-4-methoxybenzophenone (DHMB), and 2,3,4-trihydroxybenzophenone (THB)) could be found in free and conjugated forms in liver, spleen, plasma, heart, urine, and feces after oral administration (Okereke et al., 1993). The National Health and Nutrition Examination Survey 2003-2004 confirmed that exposure to oxybenzone was prevalent in the population of the United States. Nevertheless, significant concentration differences were observed according to sex and ethnicity, probably reflecting the use of cosmetic products (Calafat et al., 2008).

In the experiments presented here, oxybenzone minimized UV induced radical formation in both cell types at high concentrations. Furthermore, it also demonstrated anti-oxidative properties at base level conditions without treatment and upon AAPH-treatment. The effects were stronger in WT Fibs E6/E7 fibroblasts than in the keratinocyte cell line HaCaT. Resazurin conversion data indicate a short-term inhibition of metabolic activity. Oxybenzone is poorly soluble in aqueous solvents, which posed a limit to test it at higher concentrations. However, taking its pharmacokinetic properties and its content in commercially available sunscreen products into account, similar concentrations of oxybenzone might be found in keratinocytes and fibroblasts after application of respective products. Karsili et al. (2014) proposed that oxybenzone undergoes an electron-driven internal conversion to its keto-tautomer as an ultrafast relaxation pathway upon photoexcitation as the central mechanisms for its protective activity.

Menthyl anthranilate is an organic UVA absorber, the absorption spectrum of which shows maxima at 220 nm, 249 nm, and 340 nm (Beeby and Jones, 2000). This UV filter showed pro-oxidant as well as phototoxic effects upon UV irradiation in both cell types already at relatively low concentrations, especially if compared to those used in commercially available sunscreens. Beeby and Jones (2000) demonstrated that following 355 nm excitation the molecule converts to the triplet state. The latter can be quenched by oxygen, which subsequently leads to the generation of singlet oxygen. UV-protection implies the innoxious dissipation of the irradiation energy. Fibroblasts reacted more sensitively than keratinocytes. While the direction of effect upon UV irradiation was the same in both cell lines, menthyl anthranilate reduced AAPH-induced and baseline ROS levels in fibroblasts, while in keratinocytes the effect was the opposite.

The organic broad-spectrum ecamsule has its absorption maximum at 344 nm. Therefore, it needs to be combined with other UV filters to ensure full protection within the entire UV range. It is used after neutralization as a salt and its hydrophilic nature should prevent extensive systemic absorption after topical application *in vivo*, though metabolites were detected in the urine (Benech-Kieffer et al., 2003). Considering the maximum allowed concentration of ecamsule in sunscreens, a remarkable amount is applied in the top layers of the skin, which will somewhat decrease due to wash-off effects, e.g., due to transpiration. In the presented study, ecamsule exhibited significant protection against UV induced oxidative stress mainly in the fibroblast, where it also lowered endogenous and AAPH-induced ROS levels, though under the latter conditions the antioxidative effect was less pronounced.

The assay system proposed here can be used to demonstrate the capacity of compounds to counteract UV induced oxidative stress, thereby protecting from early events of UV damage. Several different radicals and other mechanisms contribute to UV stress; thus, it is not sufficient to investigate the scavenging activity towards, e.g., peroxyl radicals, only. While oxybenzone and ecamsule were able to reduce the oxidative stress load in these experiments, menthyl anthranilate treatment led even to an increase, mainly after UV exposure. Interestingly, quercetin was active at much lower concentrations compared to the UV filters.

To circumvent the risk of skewing results due to potential unspecific interferences of the test compounds with the indicator dye resazurin, the viability was estimated post-treatment only, after several washing steps, in the presented setup. So far, very lipophilic compounds were not investigated. However, this would be possible if they were integrated in a standardized emulsion. All experiments were performed with two cell lines from unrelated healthy human donors, originating from different relevant cell types, i.e., fibroblasts and keratinocytes. Yet, any 2D-based cell culture assay has limitations as coordinated responses of different cell layers cannot be reflected, which may be of consequence if metabolic inactivation requires the enzymatic repertoire of more than one cell type.

The fibroblasts were more sensitive to both UV and AAPH exposure compared to HaCaT cells when addressing the amount of ROS formation (Fig. 1d). Regarding the effect on resazurin reduction, fibroblasts seemed to be less sensitive than keratinocytes at 24 h post-treatment (Fig. 1f), while differences were not significant 1 h post-treatment, or for AAPH exposure at both time points. Moreover, the percentages of apoptotic/dead cells did not differ in UV treated fibroblasts compared to keratinocytes after 24 h, pointing towards decelerated metabolism rather than increased cell death. In line with our observation, Marionnet et al. showed that UV radiation related oxidative stress responses were faster in fibroblasts than in keratinocytes and differed also qualitatively (Marionnet et al., 2010). Such variations in response time could be tracked in more detail with additional time course

experiments. Moreover, substance specific pathway perturbations may also interfere with ROS and stress signaling mechanisms in an additive, synergistic, or antagonistic manner. To decipher such interactions in every detail was beyond the scope of the here presented screening approach.

To summarize, the combined safety and efficacy testing of UV filters is a pragmatic and resource-saving approach to sort out ineffective compounds at an early stage of development, to point out the need of further investigations, and/or to generate new hypotheses to be tested.

5 Conclusion

This assay provides a fast, reliable, and cost-effective screening system, which covers critical events responsible for both photoprotection and photoaging/phototoxicity, depending on the direction of the perturbation. Data show remarkable differences in the mode of action of chemical UV filters, ranging from protective to inactive to pro-oxidative properties. Although a direct extrapolation of these findings to the *in vivo* situation is not possible, the results strongly point towards the need for a more detailed mode of action-based analysis for chemical UV filters.

References

Armeni, T., Damiani, E., Battino, M. et al. (2004). Lack of in vitro protection by a common sunscreen ingredient on UVA-induced cytotoxicity in keratinocytes. *Toxicology 203*, 165-178. doi:10.1016/j.tox.2004.06.008

Baker, L. A., Horbury, M. D., Greenough, S. E. et al. (2015). Broadband ultrafast photoprotection by oxybenzone across the UVB and UVC spectral regions. *Photochem Photobiol Sci 14*, 1814-1820. doi:10.1039/C5PP00217F

Beeby, A. and Jones, A. E. (2000). The photophysical properties of menthyl anthranilate: A UV-A sunscreen. *Photochem Photobiol 72*, 10-15.

Benech-Kieffer, F., Meuling, W. J. A., Leclerc, C. et al. (2003). Percutaneous absorption of Mexoryl SX® in human volunteers: Comparison with in vitro data. *Skin Pharmacol Appl Skin Physiol 16*, 343-355. doi:10.1159/000072929

Boukamp, P., Petrussevska, R. T., Breitkreutz, D. et al. (1988). Normal keratinization in a spontaneously immortalized aneuploid human keratinocyte cell line. *J Cell Biol 106*, 761-771. doi:10.1083/jcb.106.3.761

Bruls, W. A., Slaper, H., van der Leun, J. C. and Berrens, L. (1984). Transmission of human epidermis and stratum corneum as a function of thickness in the ultraviolet and visible wavelenghts. *Photochem Photobiol 40*, 485-494. doi:10.1111/j.1751-1097.1984.tb04622.x

Calafat, A. M., Wong, L. Y., Ye, X. et al. (2008). Concentrations of the sunscreen agent benzophenone-3 in residents of the United States: National health and nutrition examination survey 2003-2004. *Environ Health Perspect 116*, 893-897. doi:10.1289/ehp.11269

Chou, T. C. and Talalay, P. (1984). Quantitative analysis of dose-effect relationships: The combined effects of multiple drugs or enzyme inhibitors. *Adv Enzyme Regul 22*, 27-55. doi:10.1016/0065-2571(84)90007-4

de Gruijl, F. and van der Leun, J. C. (2000). Environment and health: 3. Ozone depletion and ultraviolet radiation. *CMAJ 163*, 851-855.

EC – European Commission (2009). Regulation (EC) No 1223/2009 of the European Parliament and of the Council of 30 November 2009 on cosmetic products. *Off J Eur Union L 342*.. https://bit.ly/2GQ0o2n (accessed 02.08.2018).

Fourtanier, A., Moyal, D. and Seité, S. (2008). Sunscreens containing the broad-spectrum UVA absorber, Mexoryl SX, prevent the cutaneous detrimental effects of UV exposure: A review of clinical study results. *Photodermatol Photoimmunol Photomed 24*, 164-174. doi:10.1111/j.1600-0781.2008.00365.x

Health Canada (2012). Draft: Guidance Document Sunscreen Monograph. Health Products and Food Branch. https://bit.ly/2Aeg1dV (accessed 02.08.2018).

Huang, X. X., Scolyer, R. A., Abubakar, A. and Halliday, G. M. (2012). Human 8-oxoguanine-DNA glycosylase-1 is downregulated in human basal cell carcinoma. *Mol Genet Metab 106*, 127-130. doi:10.1016/j.ymgme.2012.02.017

IARC – International Agency for Research on Cancer (1992). IARC Working Group on the Evaluation of Carcinogenic Risks to Humans, World Health Organization, International Agency for Research on Cancer (1992) Solar and ultraviolet radiation, IARC monographs on the evaluation of carcinogenic risks to humans. Geneva, Switzerland.

ISO – International Organization for Standardization (2010). Cosmetics – Sun protection test methods – In vivo determination of the sun protection factor (SPF). ISO24444:2010. https://www.iso.org/standard/46523.html (accessed 18.07.2018).

ISO (2011). Cosmetics – Sun protection test methods – In vivo determination of sunscreen UVA protection. ISO 24442:2011. https://www.iso.org/standard/46521.html (accessed 01.08.2018).

ISO (2012). Determination of sunscreen UVA photoprotection in vitro. ISO 24443:2012. https://www.iso.org/standard/46522.html (accessed 01.08.2018).

Karsili, T. N., Marchetti, B., Ashfold, M. N. and Domcke, W. (2014). Ab initio study of potential ultrafast internal conversion routes in oxybenzone, caffeic acid, and ferulic acid: Implications for sunscreens. *J Phys Chem A 118*, 11999-12010. doi:10.1021/jp507282d

Klein, A., Wrulich, O. A., Jenny, M. et al. (2013). Pathway-focused bioassays and transcriptome analysis contribute to a better activity monitoring of complex herbal remedies. *BMC Genomics 14*, 133. doi:10.1186/1471-2164-14-133

Krutmann, J. (2000). Ultraviolet A radiation-induced biological effects in human skin: Relevance for photoaging and photodermatosis. *J Dermatol Sci 1,* S22-26. doi:10.1046/j.1365-2230.2000.00700.x

Leiter, U., Eigentler, T. and Garbe, C. (2014). Epidemiology of skin cancer. *Adv Exp Med Biol 810*, 120-140. doi:10.1007/978-1-4939-0437-2_7

Maini, S., Fahlman, B. M. and Krol, E. S. (2015). Flavonols protect against UV radiation-induced thymine dimer formation

in an artificial skin mimic. *J Pharm Pharm Sci 18*, 600-615. doi:10.18433/J34W39

Marionnet, C., Pierrard, C., Lejeune, F. et al. (2010). Different oxidative stress response in keratinocytes and fibroblasts of reconstructed skin exposed to non extreme daily-ultraviolet radiation. *PLoS One 5*, e12059. doi:10.1371/journal.pone.0012059

Marionnet, C., Tricaud, C. and Bernerd, F. (2014). Exposure to non-extreme solar UV daylight: Spectral characterization, effects on skin and photoprotection. *Int J Mol Sci 16*, 68-90. doi:10.3390/ijms16010068

Meinhardt, M., Krebs, R., Anders, A. et al. (2008). Wavelength-dependent penetration depths of ultraviolet radiation in human skin. *J Biomed Opt 13*, 044030. doi:10.1117/1.2957970

Nimse, S. B. and Pal, D. (2015). Free radicals, natural antioxidants, and their reaction mechanisms. *RSC Adv 5*, 27986-28006. doi:10.1039/C4RA13315C

Okereke, C. S., Kadry, A. M., Abdel-Rahman, M. S. et al. (1993). Metabolism of benzophenone-3 in rats. *Drug Metab Dispos Biol Fate Chem 21*, 788-791.

OECD (2004). Test No. 432: In Vitro 3T3 NRU Phototoxicity Test. *OECD Guidelines for the Testing of Chemicals, Section 4*. OECD Publishing, Paris, France.

Rushworth, G. F. and Megson, I. L. (2014). Existing and potential therapeutic uses for N-acetylcysteine: The need for conversion to intracellular glutathione for antioxidant benefits. *Pharmacol Ther 141*, 150-159. doi:10.1016/j.pharmthera.2013.09.006

Ryan, K. G., Markham, K. R., Bloor, S. J. et al. (2008). UVB radiation induced increase in quercetin: Kaempferol ratio in wild-type and transgenic lines of Petunia. *Photochem Photobiol 68*, 323-330. doi:10.1111/j.1751-1097.1998.tb09689.x

Ryu, J., Park, S. J., Kim, I. H. et al. (2014). Protective effect of porphyra-334 on UVA-induced photoaging in human skin fibroblasts. *Int J Mol Med 34*, 796-803. doi:10.3892/ijmm.2014.1815

Sarveiya, V., Risk, S. and Benson, H. A. (2004). Liquid chromatographic assay for common sunscreen agents: Application to in vivo assessment of skin penetration and systemic absorption in human volunteers. *J Chromatogr 803*, 225-231. doi:10.1016/j.jchromb.2003.12.022

SCCS – Scientific Committee on Consumer Safety (2018). The SCCS Notes of Guidance for the Testing of Cosmetic Ingredients and their Safety Evaluation. 10th Revision, Section 3-4.12.1. October 2018

US FDA (2018). Sunscreen drug products for over-the counter human use. Code of Federal Regulations, Title 21 – Food and Drugs, § 352.70-77. https://bit.ly/2FjX65Z (accessed 02.08.2018).

van Tonder, A., Joubert, A. M. and Cromarty, A. D. (2015). Limitations of the 3-(4,5-dimethylthiazol-2-yl)-2,5-diphenyl-2H-tetrazolium bromide (MTT) assay when compared to three commonly used cell enumeration assays. *BMC Res Notes 20*, 47. doi:10.1186/s13104-015-1000-8

WHO – World Health Organization (2018). Skin Cancers. WHO-homepage. http://www.who.int/uv/faq/skincancer/en/index1.html (accessed 18.07.2018).

Wolfe, K. L. and Liu, R. H. (2007). Cellular antioxidant activity (CAA) assay for assessing antioxidants, foods, and dietary supplements. *J Agric Food Chem 55*, 8896-8907. doi:10.1021/jf0715166

Conflict of interest

The authors declare that they have no conflict of interest.

Acknowledgement